EC
Journals.ASM.org

Delta-Aminolevulinate-Induced Host-Parasite Porphyric Disparity for Selective Photolysis of Transgenic *Leishmania* in the Phagolysosomes of Mononuclear Phagocytes: a Potential Novel Platform for Vaccine Delivery

Sujoy Dutta,[a] Celia Chang,[b] Bala Krishna Kolli,[a] Shigeru Sassa,[c] Malik Yousef,[b] Michael Showe,[b] Louise Showe,[b] and Kwang-Poo Chang[a]

Department of Microbiology/Immunology, Chicago Medical School/RFUMS, North Chicago, Illinois, USA[a]; The Wistar Institute, Philadelphia, Pennsylvania, USA[b]; and The Rockefeller University, New York, New York, USA[c]

Leishmania **double transfectants (DTs) expressing the 2nd and 3rd enzymes in the heme biosynthetic pathway were previously reported to show neogenesis of uroporphyrin I (URO) when induced with delta-aminolevulinate (ALA), the product of the 1st enzyme in the pathway. The ensuing accumulation of URO in DT promastigotes rendered them light excitable to produce reactive oxygen species (ROS), resulting in their cytolysis. Evidence is presented showing that the DTs retained wild-type infectivity to their host cells and that the intraphagolysosomal/parasitophorous vacuolar (PV) DTs remained ALA inducible for uroporphyrinogenesis/photolysis. Exposure of DT-infected cells to ALA was noted by fluorescence microscopy to result in host-parasite differential porphyrinogenesis: porphyrin fluorescence emerged first in the host cells and then in the intra-PV amastigotes. DT-infected and control cells differed qualitatively and quantitatively in their porphyrin species, consistent with the expected multi- and monoporphyrinogenic specificities of the host cells and the DTs, respectively. After ALA removal, the neogenic porphyrins were rapidly lost from the host cells but persisted as URO in the intra-PV DTs. These DTs were thus extremely light sensitive and were lysed selectively by illumination under nonstringent conditions in the relatively ROS-resistant phagolysosomes. Photolysis of the intra-PV DTs returned the distribution of major histocompatibility complex (MHC) class II molecules and the global gene expression profiles of host cells to their preinfection patterns and, when transfected with ovalbumin, released this antigen for copresentation with MHC class I molecules. These** ***Leishmania*** **mutants thus have considerable potential as a novel model of a universal vaccine carrier for photodynamic immunotherapy/immunoprophylaxis.**

Exposure of aerobic eukaryotic cells to exogenous delta-aminolevulinate (ALA) is known to trigger overproduction of porphyrins, i.e., uroporphyrins (URO), coproporphyrins (COPRO), and protoporphyrin IX (PROTO), intermediates in the heme biosynthetic pathway (31). Since all porphyrins when exposed to light generate cytolytic reactive oxygen species (ROS), ALA has been used clinically to produce endogenous porphyrins for photolytic elimination of unwanted or pathological cells or tissues, e.g., photodynamic therapy for skin tumors (21, 40). Although ALA-induced elevation of porphyrins is often low and transient in mammalian cells, there are several advantages to this approach instead of direct administration of porphyrins or other photosensitizers. ALA is a natural metabolite that participates mainly in porphyrin biosynthesis and is nontoxic even when used at a high concentration. It is also relatively stable, highly water soluble, and readily taken up by cells. These properties of ALA present a favorable profile of bioavailability for its use in photodynamic therapy (19).

Heme auxotrophs, e.g., the trypanosomatid protozoa, do not convert exogenously supplied ALA to porphyrins when the heme biosynthetic pathway is either absent or incomplete (26, 30, 36). Among these single-cell parasites, *Leishmania* spp. are functionally missing at least 5 and very possibly 7 of the 8 enzymes needed to complete heme biosynthesis (9, 30). The substantial loss of this pathway from these organisms is thought to result from their evolution of parasitism in heme-rich environments, i.e., the gut of blood-sucking insect vectors and the phagolysosomes of mononuclear phagocytes in the mammalian reticuloendothelial system (3, 4). The *Leishmania* defects in heme biosynthesis have been partially defined functionally by genetic complementation of the extracellular promastigote stage *in vitro* (9, 30). Transfection of these cells with mammalian cDNAs that express the 2nd and 3rd enzymes in this pathway results in their accumulation of URO I in response to exogenously provided ALA, the product of the 1st enzyme in heme biosynthesis (30). The immediate product expected is porphobilinogen (PBG), which in the absence of the downstream enzyme, i.e., uroporphyrinogen cosynthase, condenses and cyclizes spontaneously to form URO I instead of URO III (31). URO I is a nonmetabolizable by-product that is water soluble and is released without reuptake by cells, including *Leishmania* (10). When exposed to light, uroporphyric promastigotes are lysed, as the cytosolic URO is excited to generate singlet oxygen and other leishmanolytic ROS (10).

Received 25 August 2011 Accepted 25 January 2012
Published ahead of print 3 February 2012
Address correspondence to Kwang-Poo Chang, kwangpoo.chang@rosalindfranklin.edu.
This paper is dedicated to Shigeru Sassa in memory of his contributions and support.
Supplemental material for this article may be found at http://ec.asm.org.

doi:10.1128/EC.05202-11

Here, we extend the observation of ALA-inducible uroporphyrinogenesis/photolysis of *Leishmania* double transfectants (DTs) from the promastigotes to their intracellular amastigotes in 2 different host cell lines, i.e., mouse J774 A1 macrophages and mouse fetal skin dendritic cells (FSDC), and in primary cultures of mouse peritoneal macrophages. (Uroporphyrinogenesis denotes the production of URO from 0 to a high concentration, e.g., ~2 nmol/mg protein, when DTs were exposed as promastigotes to 1 mM ALA over a period of ~2 days.) Analyses of porphyrins in these samples by fluorescence microscopy and chromatography revealed that, when used to pulse-expose preinfected host cells, ALA was taken up and made available to their intraphagolysosomal/parasitophorous vacuolar DTs, in which URO was produced and persisted preferentially, thereby sensitizing them for selective photolysis. Photolysis of the intracellular DTs freed the major histocompatibility complex (MHC) class II molecules of macrophages from *Leishmania* sequestration in phagolysosomes, released transgenically expressed ovalbumin for MHC class I copresentation, and largely returned the expression profiles of their host cells to the preinfection state. The functional recovery of the host cells by photolysis of their *Leishmania* DTs after taking up residence in the phagolysosomes underscores the potential of these mutants to serve as effective carriers of drugs/vaccines for efficient activation and processing in these cells.

MATERIALS AND METHODS

Cells. *Leishmania amazonensis* (RAT/BA/74/LV78) clone 12-1 was routinely grown as promastigotes at 25°C in Medium 199 (Sigma) buffered with 25 mM HEPES to pH 7.4 and supplemented with 10% heat-inactivated fetal bovine serum (HIFBS). The uroporphyrinogenic mutants, which were doubly transfected with pX-*alad* and p6.5-*pbgd* (DTs), were placed under selective pressure to express the 2nd and 3rd enzymes in the heme biosynthetic pathway (30). Single transfectants (STs) with only one or the other cDNA, i.e., pX-*alad*+p6.5 or pX+p6.5-*pbgd* (30), were included as controls where appropriate in some experiments. All mutants were briefly grown in drug-free medium to stationary phase before being used for infection to avoid the potential cytotoxicity of the drugs being carried over to the host cells (9, 10).

Mouse J774 macrophage (27, 34) and FSDC (15) lines were both grown at 35°C in RPMI 1640 supplemented with 10% HIFBS. Peritoneal macrophages were obtained from BALB/c mice (~15 weeks old) and cultured in Dulbecco's modified Eagle's medium (DMEM) (Gibco) plus 5% HIFBS at 37°C in 5% CO_2. The mouse immature dendritic cell (DC) line DC2.4 was grown in HCM medium plus 10% HIFBS in 5% CO_2 (11).

***Leishmania* infection of macrophages and dendritic cells.** *Leishmania* infection of J774 cells and FSDC was initiated by mixing suspensions of these cells and of stationary-phase promastigotes in RPMI 1640 plus 20% HIFBS at a host-parasite ratio of 1:5 to 1:10, i.e., 10^6 host cells and 0.5×10^7 to 1×10^7 promastigotes/ml. The mixture was plated at 4 ml/25-cm^2 tissue culture (TC) flask or 2 ml/well in 6-well tissue culture plates. Infected cultures were maintained at 35°C with daily medium renewal. They and control cultures were prepared in multiple sets for experimentation under various conditions and taken at different time points for analyses. The total parasite load per culture was estimated by microscopic counting as described previously, i.e., using the following formula: total number of macrophages per flask × (average number of *Leishmania* amastigotes/host cell) × percent infected cells (12).

The primary macrophages were infected as a monolayer of adherent cells with promastigotes in DMEM plus 5% HIFBS. Peritoneal cells were first seeded at 2×10^5 cells/300 μl/chamber in 8-chamber tissue culture slides (Nunc). After incubation at 37°C in 5% CO_2 for 1 h, each chamber was washed 3 times with serum-free DMEM to remove nonadherent cells before use. These macrophages were infected at a host/parasite ratio of 1:10 for 2 to 3 h at 37°C and then washed to remove uningested parasites. The cultures were subsequently incubated at 35°C after infection and treated with mouse gamma interferon (IFN-γ) (Peprotech) at 100 U/ml for 24 h for induction of MHC class II expression (23, 24).

Delta-aminolevulinate-induced porphyrinogenesis. Infected and noninfected host cells were exposed to 1 mM ALA as described previously (10) daily for up to 3 days. This was done 2 to 3 days after infection was well established, as indicated by the virtual absence of extracellular parasites and their appearance in the typical large parasitophorous vacuoles (PVs) of the infected cultures. The cultures were washed and then chased for up to 3 days in ALA-free complete medium. All ALA-exposed cultures were incubated in the dark and, unless otherwise specified, handled under minimal light exposure until completion of the experiments.

Fluorescence microscopy and thin-layer chromatography of cellular porphyrins. Infected and noninfected cultures with and without ALA treatment were withdrawn daily. A small aliquot from each sample was examined first under phase-contrast microscopy and then for porphyrin fluorescence by using a specific filter set (10). The remaining samples ($>5 \times 10^6$ macrophages each) were solvent extracted for analysis of porphyrins by thin-layer chromatography (TLC) using carboxymethylated porphyrins (Porphyrin Products) as standards (9, 30).

Illumination of cultured cells. During medium renewal and microscopic observations, cultures were exposed by necessity to light that was either left unchanged, as usual for such routine operations, or minimized by dimming the light sources and shortening the handling time. Cultures were experimentally illuminated with white light at ~6.5 mW/cm^2 for variable time periods and at porphyrin-excitable wavelengths, i.e., long-wave UV light (λ_{max} = 366 nm), as described previously (9, 10, 30), or violet light (LumaCare probe; λ_{max} = 400 nm). Since a desirable outcome was achieved under all experimental conditions of illumination used, they are specified for individual experiments in the figure legends.

Localization of MHC class II and LAMP-1 by immunofluorescence microscopy. Peritoneal cells cultured in 8-chamber microscope tissue culture slides (Nunc) processed as described above were used. DT infection, ALA treatment, and light exposure of these cells, together with their controls, were also done as described above. Samples were taken at different times up to 16 h after induction of MHC class II expression with IFN-γ. After fixation and permeabilization with Cytoperm-Cytofix reagent (BD Biosciences) for 15 min at 4°C, samples were treated with anti-CD16/32 (1:100 dilution) in the presence of 5% bovine serum albumin (BSA) plus 5% normal rat and rabbit sera in Permwash buffer (BD Biosciences) at 4°C for 30 min. After washing 3 times with this buffer, the preparations were treated for 1 h at 4°C with a combination of fluorescein isothiocyanate (FITC)-labeled rat anti-mouse MHC class II-IgG (M5/114.15.2; Biolegend) and rabbit anti-human LAMP-1 (6) (monoclonal C-20 against the conserved C-terminal sequence; Santa Cruz Biotechnology), both at a 1:100 dilution in 0.1% saponin plus 1% bovine serum albumin in phosphate-buffered saline. After washing, the cells were further treated for 1 h at 4°C with goat anti-rabbit IgG labeled with Alexa 594 at 1:1,000 for LAMP-1. The cells were finally washed and mounted in antifade mounting medium with DAPI (4′,6-diamidino-2-phenylindole) (SlowFade; Molecular Probes). About 100 cells were examined per sample per treatment, and the data presented are representative of the overall observations.

MHC class I/OVA epitope copresentation by dendritic cells after infection with OVA-transfected DTs and their photolysis in situ. MHC class I/ovalbumin (OVA) epitope copresentation by DCs after infection with OVA-transfected DTs and their photolysis in situ is based on monoclonal antibody immunodetection of the OVA-SIINFEKL epitope/MHC class I complex copresentation in DT/OVA-infected DC2.4 cell lines, as described previously (11). Briefly, DT promastigotes were transfected with *pX63hyg-ova*, consisting of a truncated OVA (amino acids [aa] 140 to 386) cloned into the BglII expression site of *pX63hyg*. Stable transfectants were selected and grown in the presence of 500 μg/ml hygromycin. OVA expression in the transfectants was verified by Western

blotting using anti-OVA rabbit antisera (Millipore; dilution, 1:1,000). H-2Kb OVA(257–264) (SIINFEKL) complexes with MHC class I in OVA/DT-infected DCs were assessed by immunofluorescence microscopy. DC2.4 dendritic cells were exposed for 24 h in 200 μl of complete medium to the following materials: 100 pM SIINFEKL and 5 mg/ml OVA as reagent positive controls and medium alone as the negative control. OVA/DT-infected DCs with (DT OVA + ALA + light) and without (DT OVA − ALA − light) treatments for uroporphyrinogenesis/photolysis were evaluated for comparison. Non-OVA transfectants were treated similarly (DT + ALA + light) as an additional control. All cells were fixed and permeabilized and then reacted at 4°C for 16 h with the monoclonal antibody from the 25-D1.16 hybridoma culture supernatants, followed by goat anti-mouse IgG-Alexa 488 (Molecular Probes; 1:500 dilution) to assess the H-2Kb OVA(257–264) (SIINFEKL).

The filter sets used for image acquisition by fluorescence microscopy were as follows: (i) DAPI, D365/10× (365-nm exciter), 400DCLP (400-nm dichroic), and D460/50 M (460-nm emitter); (ii) FITC, HQ480/40× (480-nm exciter), Q505LP (505-nm dichroic), and HQ 535/50 M (535-nm emitter); (iii) Alexa 594, HQ 560/55× (560-nm exciter), Q595LP (595-nm dichroic), and HQ 645/75 M (645-nm emitter); and (iv) porphyrins, D405/10 (405-nm exciter), Q485DCXR (485-nm dichroic), and RG610LP (610-nm emitter) (Chroma Tech Co., Brattleboro, VT). Images were captured by using a Nikon Eclipse 80i microscope fitted with a CoolSnap ES camera in conjunction with Metamorphosis image acquisition software (version 6.2r6).

Microarray analyses. Microarray analysis was done at a single time point for different experimental and control groups when intraphagolysosomal DTs were lysed in DT-infected cells after ALA and light exposure. RNA was TRIzol extracted according to the manufacturer's protocol from the experimental and control groups (>2 × 10^6 J774 cells each) and analyzed to verify its integrity using a BioAnalyzer (Agilent). Each RNA sample (2 μg) was then amplified using the Arcturus RNA amplification kit to produce a stock of amplified mRNA (aRNA) (18). The aRNA (1.6 μg) was ^{33}P labeled and hybridized simultaneously to 4 arrays spotted with a total of 38,000 mouse cDNA clones carrying ~21,000 unique mouse genes. The cDNA filter arrays were prepared by the Wistar Institute Genomics Facility. One of the arrays, printed specifically for these studies, carried, in addition to the mouse cDNAs, *Leishmania* genes, i.e., *ndk*, *β-tub*, *nagt*, and *dhfr* (GenBank accession numbers L1648.07, M23441, M96635, and L11705), encoding nucleoside diphosphate kinase b, beta-tubulin, *N*-acetylglucosamine-1-phosphate transferase, and dihydrofolate reductase, respectively. *nagt* and *dhfr* are single-copy genes, while *β-tub* and *ndk* are multicopy genes. The expression values were determined with ImaGene software (Biodiscovery) using the median pixel for each spot and an area adjacent to the spot for background correction. Average normalized median densities (nMD) were calculated in the four replicates of each experimental condition, and the standard deviation was determined. Data were exported to Excel for further analysis (18) and transformed into corresponding *z* scores for clustering in TreeView (13). Pairwise combinations were analyzed with the *t* test. The false-discovery rate as a function of the *P* value was estimated by permuting the quadruplicate values under the two conditions being tested (37). Genes with significant expression changes were selected with a cutoff *P* value of <0.05 and then filtered to include only those genes that exhibited >2-fold change in expression.

Real-time PCR. To verify the changes in transcription profiles, duplicate samples were analyzed with TaqMan gene expression assays. The total RNA samples (3 μg) from different treatment groups were used to generate cDNAs with the GoScript Reverse Transcription system (Promega). Multiplex real-time PCR was performed with the cDNAs produced using TaqMan MGB gene expression probes for mouse *il10* (part no. 4453320; Applied Biosystems) and the housekeeping gene *gapdh* (part no. 4352339E) with 6-carboxyfluorescein (FAM) and VIC dyes, respectively, according to the manufacturer's recommendations, using the Applied Biosystems StepOne Real-Time PCR system. Data were analyzed using the comparative C_T method, where ΔC_T values were calculated by subtracting *gapdh* C_T values from those of *il10*, which were converted into linear values using the formula $2^{-\Delta CT}$.

Statistical analyses. All experiments pertaining to infection and ALA exposure/illumination for porphyrinogenesis/photolysis were repeated >10 times. All other experiments were performed at least three times each with samples in duplicate for microscopic counting of parasite loads and in triplicate or quadruplicate for the rest. Data are presented as means with standard errors calculated from multiple samples of representative experiments. Student's *t* test and one-way analysis of variance (ANOVA) were used to calculate the statistical significance of data, as described.

RESULTS

Uroporphyrinogenic *Leishmania* promastigotes (DTs) retained infectivity to their host cells. Both porphyrinogenic (DT) and nonporphyrinogenic (ST) mutants were found to infect host cells equally well by producing large PVs in 1 to 3 days (Fig. 1A to C and A′ to C′, phase-contrast), exactly as seen with their parental wild-type clone (5). During the subsequent period of incubation for 9 days or longer, the intra-PV DTs showed kinetics of parasite burden similar to those produced by the nonporphyrinogenic mutants and their parental wild type (Fig. 1D, solid and open circles versus open square), the kinetics of the host cell replication being comparable among the 3 infected cultures (Fig. 1D′). The transgene products of the DT mutants *per se* thus did not alter their infectivity to the host cells examined.

Host-parasite differential porphyrinogenesis after pulse-exposure of DT-infected cells to ALA. (i) Porphyrin fluorescence dissipated rapidly in host cells but persisted in intra-PV DTs. Cells were exposed to 1 mM ALA ~3 days after infection, when virtually all *Leishmania* promastigotes were endocytosed and thus intracellular. Porphyrin fluorescence was initially seen largely in the cytoplasm of the host cells, irrespective of their infection with DTs or STs in the presence of ALA (Fig. 1A and B, day 1 fluorescence), but not in its absence (Fig. 1C, day 1 fluorescence). These fluorescent signals thus represent the porphyrins, which the host cells overproduced from exogenously provided ALA to a level visible by fluorescence microscopy. Porphyrin fluorescence diminished with the removal of ALA in the host cells to a microscopically undetectable level and, concomitantly, emerged at variable intensities in the intra-PV DTs (Fig. 1 A′, J + DT + ALA fluorescence day 3), but not in those of the negative controls, i.e., intra-PV STs in infected and ALA-exposed cells (Fig. 1 B′, J + ST + ALA fluorescence day 3) or DTs of the infected cells not exposed to ALA (Fig. 1C′, J + DT − ALA fluorescence day 3). Taken together, the results of these studies indicate that exposure of DT-infected cells to ALA induces host-parasite differential porphyrinogenesis in time and porphyrin level.

(ii) URO persisted, while COPRO and PROTO dissipated rapidly after a transient rise in DT-infected cells. DT-infected J774 cells and controls, e.g., noninfected cells, were exposed to ALA. Samples were withdrawn daily during the subsequent chase for 3 days to evaluate porphyrin changes by TLC analysis (Fig. 2). As expected, all 3 known naturally occurring porphyrins, i.e., URO, COPRO, and PROTO (in the order of their appearance in the heme biosynthetic pathway), were present in day 1 samples of both DT-infected and noninfected host cells (Fig. 2, J + DT + ALA versus J + 0 + ALA, lane 1). PROTO was more obvious and consistent than COPRO, but their fluorescence intensities were comparable in DT-infected and noninfected cultures. URO was highly dominant in relative intensity over the other species in

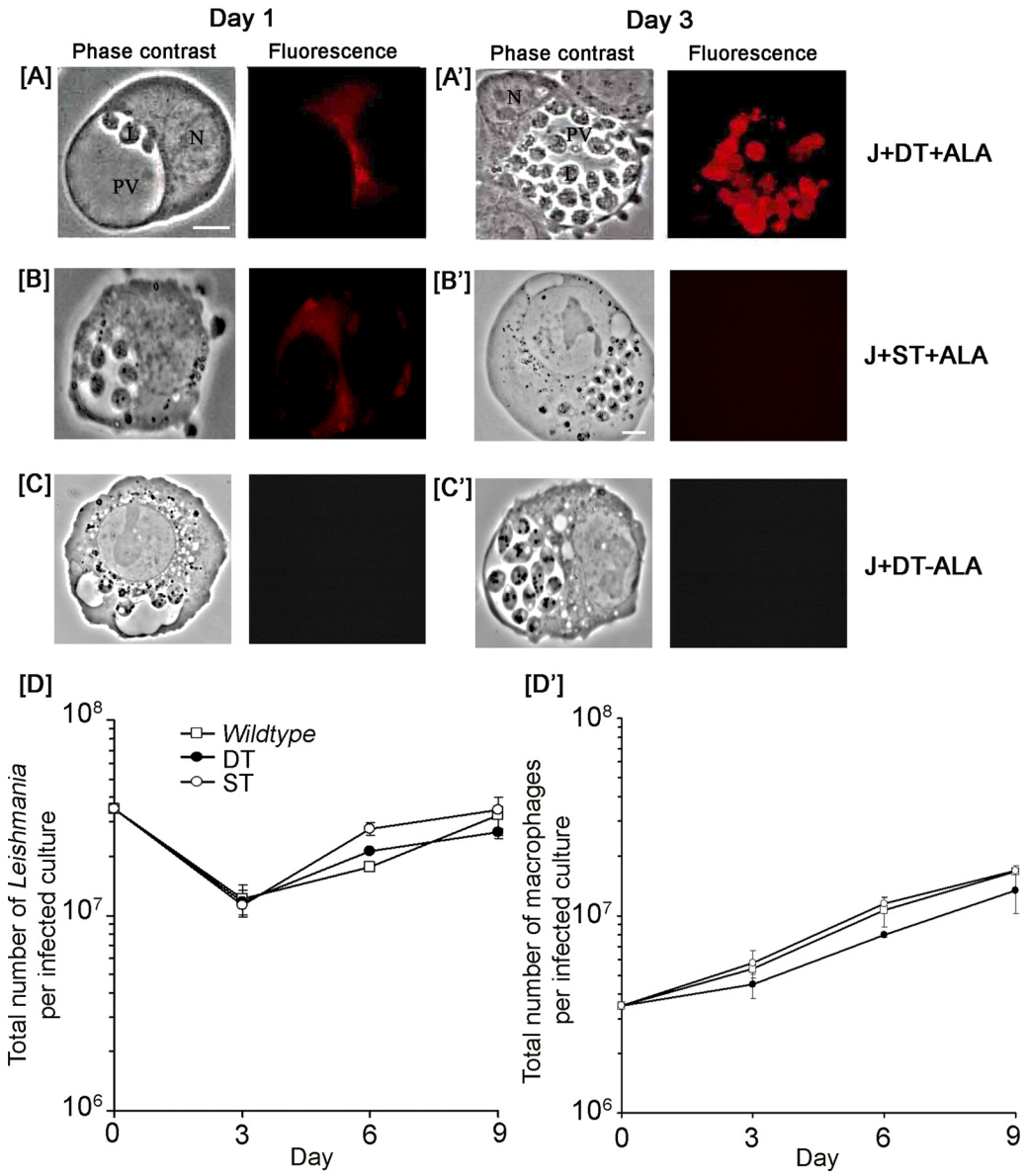

FIG 1 Host-parasite porphyric disparity after pulse-exposure of DT-infected cells to delta-aminolevulinate and equal infectivity of nonporphyric DT and ST *Leishmania* mutants to host cells. (A to C and A′ to C′) Phase-contrast (left) and porphyrin fluorescence (right) showing PVs and differences in the kinetics of porphyrinogenesis between macrophages and their *Leishmania* DT mutants after ALA pulse-exposure (Day 1) and chase (Day 3). J + DT + ALA and J + ST + ALA, J774 macrophages (J) infected with uroporphyrinogenic (DT) and nonporphyrinogenic (ST) mutants, respectively, at a ratio of 1:10 for 2 days. The infected cells were then pulsed for ~1 day with 1 mM ALA (+ ALA) (day 1) and chased in ALA-free medium for 2 more days (day 3). J + DT − ALA, macrophages infected as described above but not exposed to ALA. ST, transfectants with pX-*alad* and p6.5. Transfectants with another ST, i.e., pX and p6.5-*pbgd*, produced the same results (not shown). Scale bar = 10 μm for all panels, except B′, in which a shorter scale is provided for 10 μm. (D and D′) Kinetics of parasite loads (D) per culture of J774 cells infected with the parental wild-type, uroporphyrinogenic double transfectants and nonporphyrinogenic single transfectants and of replication of the host cells in the respective cultures (D′). The error bars indicate standard errors.

DT-infected versus uninfected cells (Fig. 2, J + DT + ALA versus J + 0 + ALA, lane 1, URO). After further chase in ALA-free medium, URO remained dominant in DT-infected cells (Fig. 2, J + DT + ALA, lanes 2 and 3), while COPRO and PROTO dissipated to levels undetectable by TLC in all cells. The URO detected by TLC in the DT-infected cells after chase originated from the intra-PV DTs, as they were the only structures that remained highly fluorescent when observed by fluorescence microscopy (Fig. 1A′, day 3). Without exposure to ALA, neither DT-infected cells nor noninfected cells (Fig. 2, J + DT − ALA and J + 0 − ALA) produced any TLC-detectable porphyrins, also consistent with the fluorescence microscope observations (Fig. 1C and C′). Comparison of DT- versus ST- or wild-type-infected cells produced the same outcome under similar experimental conditions (not shown).

The origin of the TLC-resolved URO from the intra-PV uroporphyric DTs was shown clearly by using mouse peritoneal macrophages, which were first infected with DT and then exposed to ALA under the conditions used for the cell lines. Porphyrin fluorescence was clearly visible microscopically but limited only to the

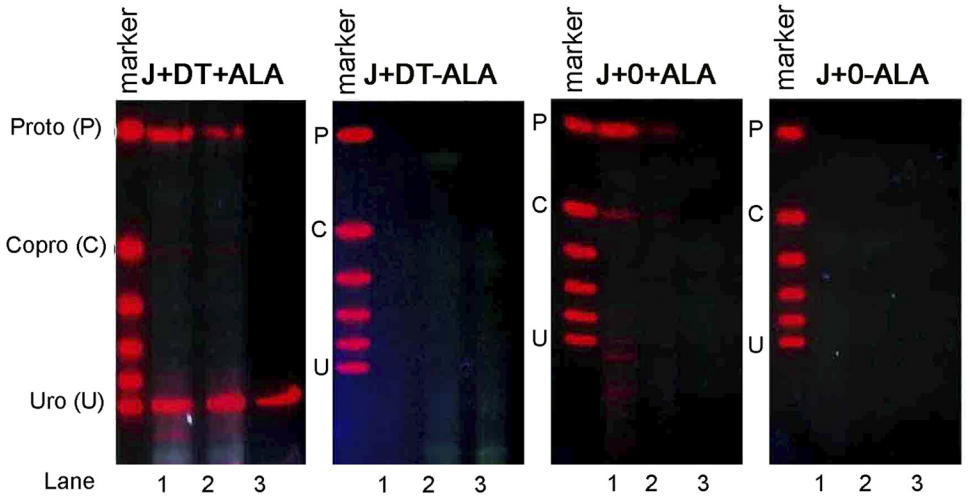

FIG 2 Chromatographic separation of porphyrins extracted from DT-infected and uninfected macrophages showing the persistent presence of URO originating from uroporphyric DT *Leishmania*. J + DT + ALA, J774 cells infected with DT for 3 days, treated with 1 mM ALA daily after 3 days, and chased for 3 more days. J + DT − ALA, omission of the ALA treatments; J + 0 + ALA, omission of DT infection; J + 0 − ALA, J774 macrophages with neither DT infection nor ALA treatment. Lanes 1 to 3, days 1 to 3 of chase after the ALA treatments. Porphyrins extracted from ~5×10^6 macrophages were loaded in each lane. Copro (C), Proto (P), and Uro (U), carboxymethylated porphyrin markers corresponding to coproporphyrins, protoporphyrin IX, and uroporphyrins.

intracellular DT (see Fig. S1A in the supplemental material). TLC analyses of the total porphyrins extracted from DT-infected peritoneal macrophages showed that URO was the sole porphyrin species visible (see Fig. S1B in the supplemental material), clearly corresponding to the fluorescent signals seen microscopically in the DTs.

The results from all 3 types of host cells used indicate that the porphyrin fluorescence seen to persist in their intra-PV DTs after exposure to ALA corresponds to TLC-resolvable URO, but not COPRO or PROTO. The last two made only a transient appearance at a relatively low level in the host cell lines, irrespective of infection or lack of infection and the *Leishmania* used for the infection.

Selective photolysis of uroporphyric DTs in the phagolysosomes of DT-infected host cells by illumination. (i) Intra-PV uroporphyric DTs were sensitive to dim light. The fact that intra-PV uroporphyric DTs were sensitive to dim light was noted initially in a preliminary study when DT-infected cultures were handled as usual under normal laboratory lighting conditions. Namely, ALA treatments of DT-infected, but not ST-infected, cultures were found to sharply decrease the intracellular amastigotes during a period of >26 days after infection, although the effectiveness decreased with time (see the legend to Fig. S2 in the supplemental material for details). By minimizing the exposure of DT-infected cells to light, the intra-PV uroporphyric DTs no longer decreased steeply, although they were still consistently fewer in number than those of the control groups, which either remained steady or increased over the period of incubation (Fig. 3A, DT + ALA versus ST + A), while the host cells were not affected (Fig. 3A′). The susceptibility of the intra-PV uroporphyric DTs to ambient/incipient light suggested by these observations predicts their high photosensitivity, which was verified by experimental illumination (see below).

(ii) Experimental illumination of DT-infected cells extensively photolysed their intra-PV uroporphyric DTs selectively. By counting parasites and host cells, i.e., J774 macrophages and FSDC of the DT-infected cultures after ALA treatment followed by experimental illumination (+ light) in comparison to the controls, i.e., ALA alone plus incipient light (+ ALA) and light alone (Fig. 4), it was shown that experimental illumination of DT-infected cells extensively photolysed their intra-PV uroporphyric DTs selectively. The decrease in the number of intra-PV porphyric versus control DTs was in the following order: + ALA + light > + ALA − light > − ALA + light (equal to untreated [not shown]) (see legends to Fig. 4A and B for the experimental-illumination conditions used). After exposure of the DT-infected cultures to both ALA (red arrow) and light (black arrow) (Fig. 4A and B, solid circles), the parasite loads decreased by 1 or 2 orders of magnitude and never recovered throughout the period of observation up to 10 to 12 days. The parasite loads decreased progressively after the combination treatments to a negligible level when the host/para-

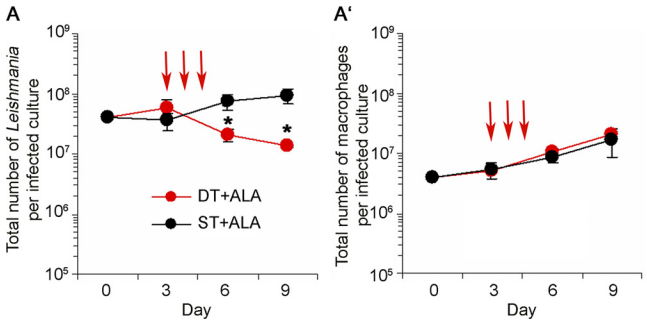

FIG 3 Depression of parasite loads in DT-infected, but not ST-infected, host cells after ALA treatments under incipient light. Shown are the kinetics of parasite loads (A) and host cell replication (A′) per culture of J774 cells infected with uroporphyrinogenic (DT) and nonporphyrinogenic (ST) mutants after exposure to ALA (+ ALA). The arrows indicate daily ALA treatments during medium renewals for 3 consecutive days from day 3 to day 5 after infection for a total period of 9 days. Statistical significance, indicated by the asterisks: $P < 0.01$, calculated using the Student *t* test. The error bars indicate standard errors.

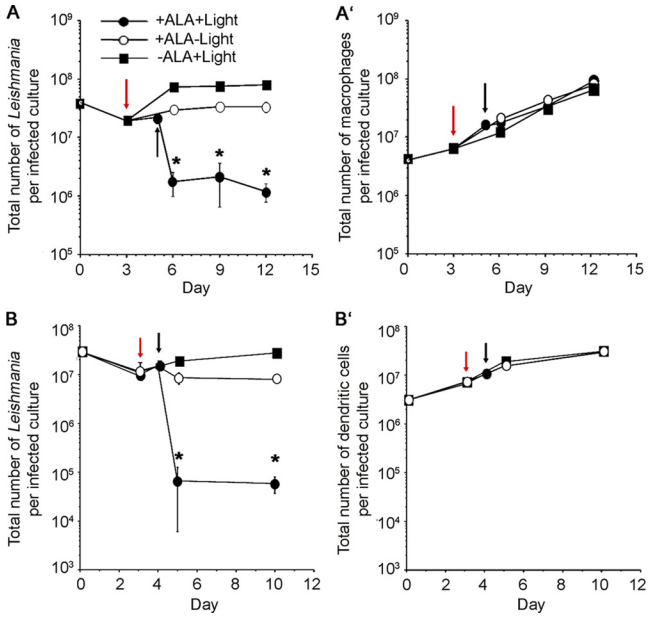

FIG 4 Significant clearance of parasite loads from DT-infected host cells after ALA treatment followed by experimental illumination. J774 macrophages (A and A′) and fetal dendritic cells (B and B′) were infected with DTs, followed by exposure to 1 mM ALA and white-light illumination for 15 min (12.15 J/cm^2). The parasite loads (A and B) and the total numbers of host cells (A′ and B′) were estimated per infected culture at the time points indicated under various conditions, as shown (± ALA ± light). The red and black arrows indicate the time points of 1× ALA treatment and light exposure, respectively. Statistical significance, denoted by the asterisks: $P < 0.001$, calculated using one-way ANOVA. The error bars indicate standard errors.

site ratios used to initiate the infection were reduced from 1:10 to 1:2 (not shown). In contrast, the intra-PV DTs increased in number in the light-alone controls (Fig. 4A and B, solid squares) and remained steady or decreased slightly in those treated with ALA alone (Fig. 4A and B, open circles). Exposure of DT-infected J774 cells to 1× ALA rather than 3× ALA was the condition used, since it appeared to have already optimally induced the uroporphyrinogenesis of intraphagolysosomal DTs (cf. Fig. 3A; see Fig. S2 in the supplemental material). None of the treatments noticeably affected the host cells, as they replicated at comparable rates under all conditions used (Fig. 4A′ and B′).

By fluorescence microscopy, URO fluorescence was seen to fill the PVs ~2 h after illumination, indicating that URO was released from the DTs, resulting apparently from the leakiness of their plasma membranes as a sign of cytolysis (Fig. 5, + ALA + light), and disintegrated beyond recognition after further incubation overnight (not shown). In contrast, the intra-PV DTs retained their integrity in the control groups (Fig. 5, − ALA + light and + ALA − light). The results obtained thus indicate that the intra-PV uroporphyric DTs are selectively susceptible to experimental illumination for elimination from infected cells.

Selective photolysis of intra-PV DTs by pulse-exposure of infected cells to ALA followed by experimental illumination returned their host cells to their preinfection status. (i) Photolysis of intraphagolysosomal DTs released MHC class II sequestration by *Leishmania*. Mouse peritoneal macrophages were used for photolysis of intraphagolysosomal DTs, since they were more readily inducible with IFN-γ to express MHC class II molecules than the J774 cells. After infection of these macrophages with DT (Fig. 6A, DT − ALA + light), MHC class II molecules (green) were visualized only in discrete sections of the PV membrane,

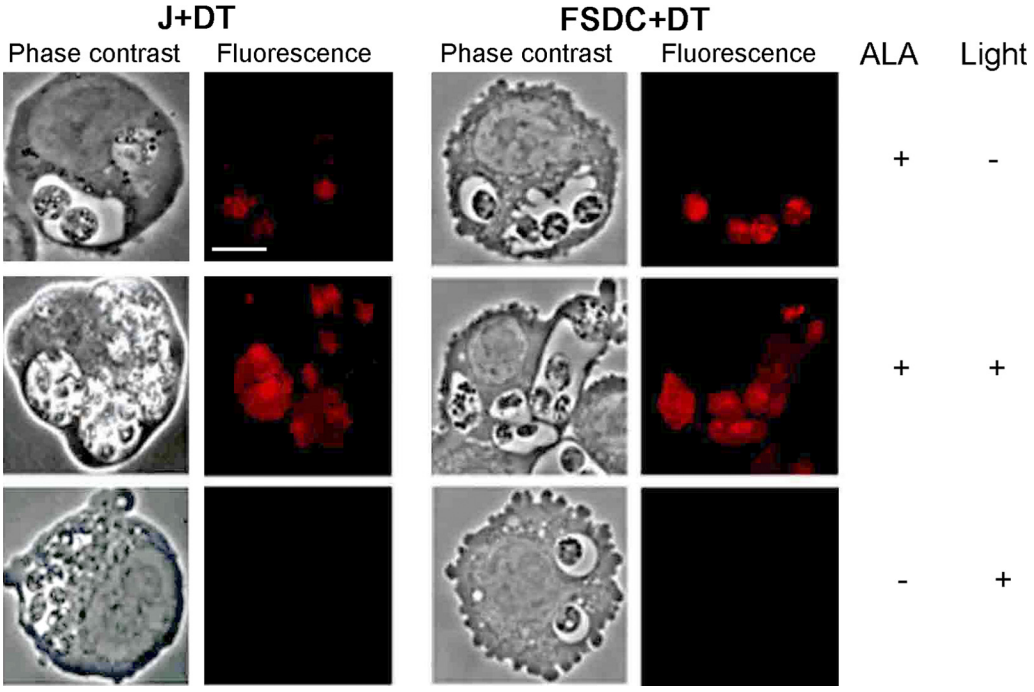

FIG 5 Selective photolysis of intra-PV uroporphyric DTs after experimental illumination of DT-infected host cells. Shown are phase-contrast (left) and porphyrin fluorescence (right) microscopy of uroporphyrinogenic-DT-infected J774 macrophages (J + DT) and fetal skin dendritic cells (FSDC + DT) with and without 1 mM ALA exposure and/or white-light illumination for 15 min (12.15 J/cm^2), as indicated (± ALA ± light). The cells were examined 2 h after illumination. Scale bar = 10 μm.

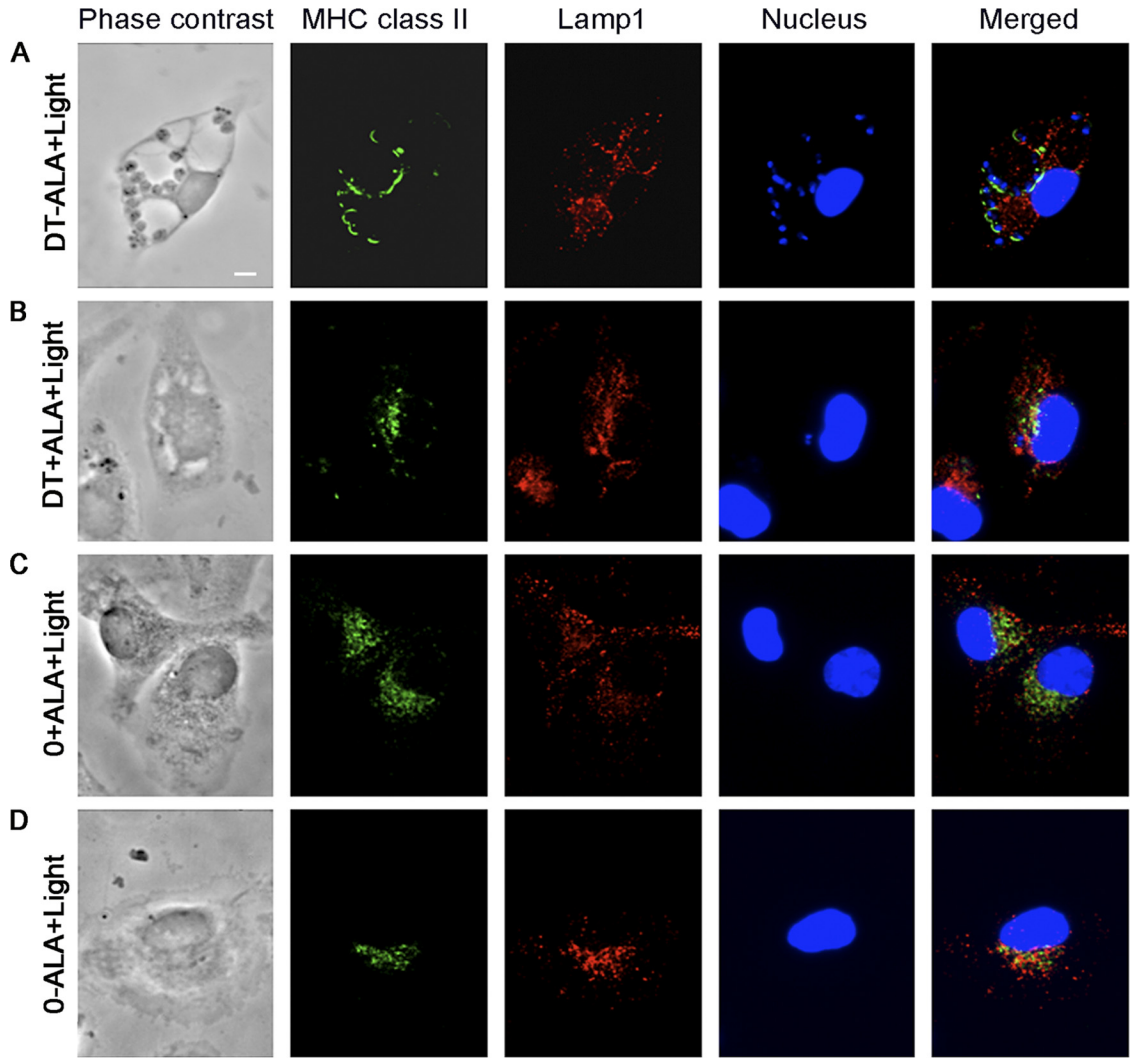

FIG 6 Recruitment of MHC class II molecules to LAMP-1-positive PVs after infection of mouse peritoneal macrophages with DTs and their return to normal distribution after photolysis of intra-PV DTs. Mouse peritoneal macrophages (Phase contrast) infected with uroporphyrinogenic mutants (+ DT) (A and B) and uninfected controls (C and D) were exposed to IFN-γ to induce MHC class II expression. One set, consisting of infected (B) and uninfected (C) cells, was exposed to the conditions for selective photolysis of intra-PV uroporphyric DTs, i.e., treatment with 1 mM ALA overnight (+ ALA) followed by illumination (400 nm) at 7.5 J/cm^2 (+ light). The remaining set of infected (A) and uninfected (D) cells served as porphyrin-free and thus nonphotolytic controls. A monolayer of all cell samples (A to D) was further incubated for 2 h after photolytic treatments before processing for localization of MHC class II (green), LAMP-1 (red), and the nucleus (blue) by immunofluorescence microscopy. See Materials and Methods for experimental details. Scale bar = 10 μm.

which were delineated by the lysosomal marker, i.e., LAMP-1 (red). Adhesion of amastigotes to the PV membrane was evident (phase-contrast) and was made obvious by DAPI staining of their nuclei (blue). The merged image suggested that the MHC class II molecules were often sequestered in the intervening region between the amastigote membrane and the vacuolar membrane and were absent in the remaining portion of the large PV free of amastigote attachment. When observed ≥2 h after exposure of the DT-infected macrophages to ALA + light, PVs were found to become smaller and contained disintegrating DTs (Fig. 6B, phase-contrast). MHC class II (green) and LAMP-1 (red) molecules became dispersed, approaching the distribution seen in the noninfected controls (Fig. 6C and D, 0 + ALA + light and 0 − ALA + light). Upon further incubation for up to 16 h (see Fig. S3 in the supplemental material), the distribution of the MHC class II molecules (green) became indistinguishable between the infected cultures after DT photolysis (see Fig. S3, DT + ALA + light) and noninfected cells (see Fig. S3, controls). In contrast, DT-infected macrophages treated with ALA alone in the dark continued to harbor intact, DAPI-positive, and vacuolar-membrane-attached amastigotes (yellow) in large PVs (see Fig. S3, DT + ALA − light). Photolysis of intra-PV porphyric DTs thus released the sequestered MHC class II molecules and restored their normal cellular distribution in the host cells.

(ii) Expression profiles of the host cells returned to normal after photolysis of their intra-PV DTs. The cDNA microarray analyses of DT-infected J774 cells versus the control groups showed that photolysis of the intra-PV DTs reversed the effect of their infection on the host cells more generally than just releasing the sequestration of their MHC class II molecules. The global transcription profile of the host cells became more similar to their preinfection state after photolytic suppression of the infection. The microarray data are presented here to illustrate this point. DT

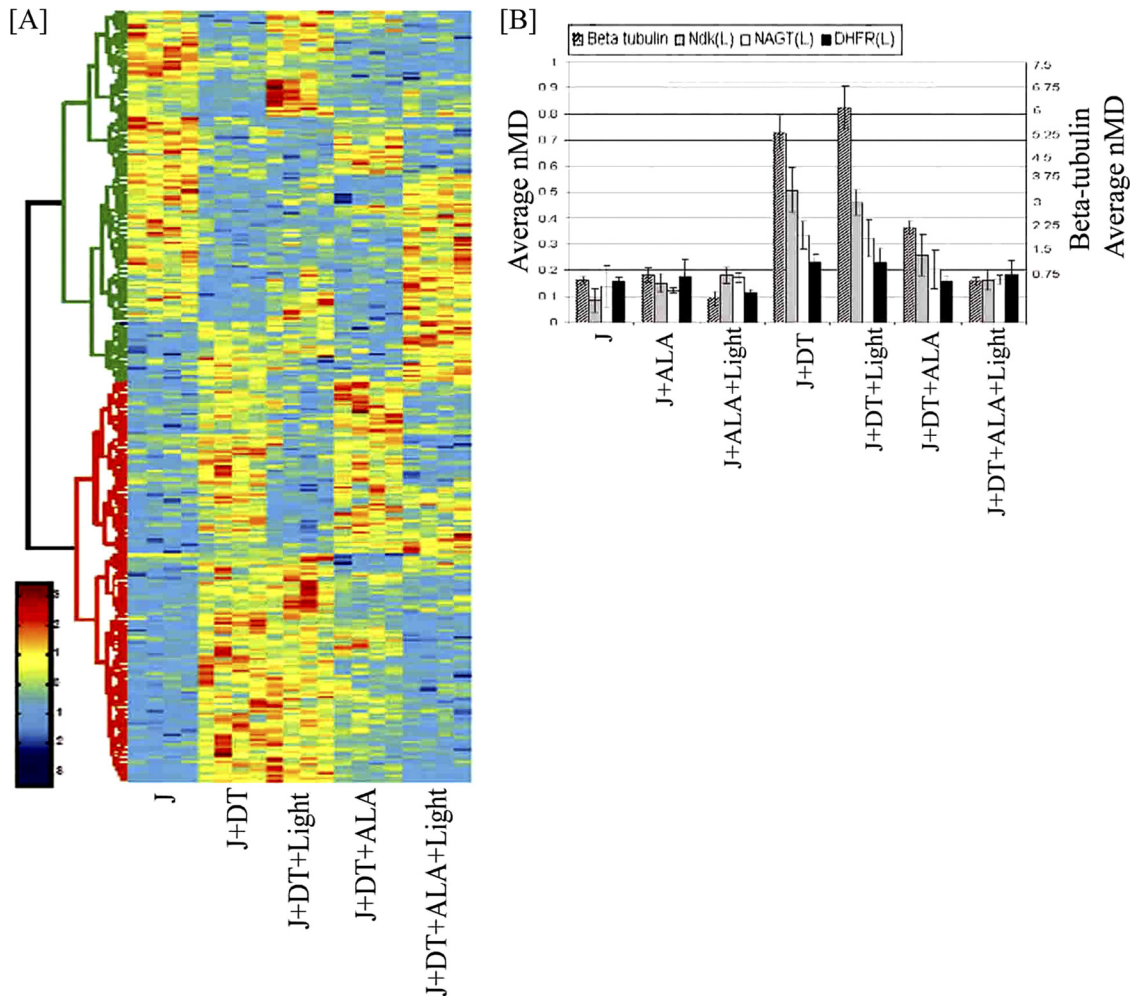

FIG 7 Macrophage and *Leishmania* expression profiles of DT-infected cells after ALA-induced porphyrinogenesis and selective photolysis of intra-PV uroporphyric DTs. J, J774 macrophages; J + DT, J774 cells infected with DTs; J + DT + light, illumination of DT-infected cells with a long-wave UV lamp (λ_{max} = 366 nm) for 10 min; J + DT + ALA, treatment of J + DT with 1 mM ALA for 16 h; J + DT + ALA + light, exposure of J + DT to both ALA and light, followed by chase in ALA-free medium for 3 days. All samples were subjected to microarray analysis (~21,000 mouse genes plus 4 *Leishmania* genes) (see Materials and Methods for details). (A) Hierarchical clustering of genes showing their expression patterns in DT-infected cells versus uninfected cells and subsequent changes that occur upon induction of *Leishmania* photolysis. A total of 3,102 macrophage genes showed altered expression ($P < 0.05$) compared to uninfected (J) and infected (J + DT) macrophages. The 318 clustered genes shown here had >2-fold changes in the expression levels in at least one of the treatments (J + DT + ALA, J + DT + light, and/or J + DT + ALA + light) in comparison to J + DT. The expression levels of these 318 genes in uninfected J cells (J) are included for reference to the preinfection expression patterns for these genes. The color scale indicates the change for each gene based on median intensity (pale green) from downregulated (dark blue to light blue) to upregulated (yellow to red) for each condition using units of *Z* (standard deviations). Gene clustering is indicated at left, with two principal families: red, those which start low, increase, and then return to low initial values; and green, those which start high, decrease, and then rise to initial values. (B) Progressive decrease of *Leishmania* DT-specific gene expression from ALA-induced uroporphyrinogenesis of DTs and their photolysis in infected host cells. The four *Leishmania* genes spotted in triplicate on the arrays were used to assess the effects of various treatments on the protozoan transcription as a measure of their persistence. The average normalized medium densities (nMD) for three individual spots for each of the four genes in the four replicate experiments were used to plot the expression levels. *Leishmania ndk*, *nagt*, and *dhfr* genes are plotted on the left-hand scale, and beta-tubulin is on the right-hand scale (1st bar of the 4 for each treatment group). The beta-tubulin value is higher, presumably resulting from cross-hybridization of the *Leishmania* probe with sequence-conserved murine beta-tubulin messages inherently abundant in macrophages. The error bars indicate standard errors.

infection of macrophages was found to alter the expression of the 3,102 genes at a *P* value of <0.05, i.e., ~15% of the ~21,000 unique clones. The list was reduced to 247 when it was filtered to include only those with a *P* value of <0.01 and with >2-fold change. Changes in expression levels ranged from up 900-fold to down 200-fold (Fig. 7A, J + DT versus J). Table S1 in the supplemental material lists the most significant 100 genes (by *P* value) that changed after infection. The effects of treatments with ALA and light under different conditions on the DT-infected cells were assessed by one-way ANOVA within the 3,102 genes ($P < 0.05$) that had their expression levels altered by the infection. Figure 7A shows hierarchical clustering of the 318 genes that had their expression levels further altered after treatments of the infected cells. Light alone (J + DT + light) had some effect on gene expression that was unrelated to the phenotypes under study. However, ALA, and especially ALA + light, resulted in a more significant reversal of the infection-produced changes in gene expression of the macrophages (see Table S2 in the supplemental material for a gene list). These changes before and after uroporphyrinogenesis/photolysis were verified by reverse transcription (RT)-PCR for inter-

leukin 10 (IL-10) (see Fig. S4 in the supplemental material). Photolytic disruption of the active infection returned the expression of many downregulated and upregulated genes to baseline uninfected levels. This is more obvious for the genes upregulated than for those downregulated by infection.

Photolytic suppression of DTs in infected macrophages is indicated by the changes in the expression of the 4 *Leishmania* genes included in the arrays (*beta-tubulin*, *nagt*, *ndk*, and *dhfr*) upon infection and then as a function of the treatments (Fig. 7B). The expression of all 4 *Leishmania* genes increased with infection. The levels of the *Leishmania* transcripts were unaffected by exposure of the infected cells to illumination alone (J + DT + light = J + DT) but were reduced by ALA treatment (J + DT + ALA) and subsequently returned to the background of no infection when further experimentally illuminated with light (J + DT + ALA + light). Transcription of intra-PV DTs was reduced with uroporphyrinogenesis upon ALA treatment and completely absent after exposure to experimental illumination for photolysis.

The results of the microarray analyses support the conclusion that the intra-PV DTs are selectively affected, reversing the inhibition of their host cells by the infection.

Uroporphyrinogenesis/photolysis of DTs released antigens in dendritic cells for MHC class I copresentation. OVA released from the OVA-expressing DTs via uroporphyrinogenesis/photolysis in the DCs was apparently processed correctly by these antigen-presenting cells (APCs) to present the known MHC class I-specific SIINFEKL epitope. This is indicated by the positive reaction of this MHC class I-epitope complex with a specific monoclonal antibody, 25-D1.16 (see Fig. S5 in the supplemental material). The positive immunoreaction products (green or pale blue when overlapped over DAPI-stained nuclei) were present in DCs infected with DT OVA after their photolysis *in situ* (see Fig. S5, [+ DT OVA] + ALA + light), but not with these mutants without photolysis (see Fig. S5, [+ DT OVA] − ALA − light) or control DTs with photolysis ([+ DT] + ALA + light). The level of the positive reactivity, however, was weaker than for those exposed to SIINFEKL or OVA (see Fig. S5, left, + SIINFEKL peptides, + OVA).

DISCUSSION

The present study provides the first demonstration of the new proposed approach to photodynamic medicine (30), showing that ALA exposure of host cells preinfected with transgenic *Leishmania* induces the neogenesis and accumulation of URO to an exceptionally high level in these intracellular parasites (Fig. 1A′). Previously, a partial rescue of *Leishmania*'s natural defects in heme biosynthesis by forward genetics was shown to make this possible in the extracellular stage, i.e., DT promastigotes (10, 30). Uroporphyrinogenesis is triggered by exposure of these promastigotes to ALA, indicative of its cellular uptake. Surprisingly, exposure of the DT-infected macrophages to ALA also readily elicits uroporphyrinogenesis in their DT amastigotes despite the intra-PV residence of the latter. The ALA, which is imported into the PVs of the host cells via their pinocytic activity (unpublished data), appears to provide the substrate that is used to initiate this response by the DT parasite. This is strongly supported by the exclusion of the likely alternative ALA sources from the cells, since *Leishmania* lacks the ALA synthase needed to produce this substrate (9), and the host cells, i.e., macrophages and dendritic cells, as nonerythrocytic cells, stringently regulate ALA synthase as a rate-limiting enzyme in their heme biosynthetic pathway (17, 32). While the exact mechanism for the uptake of exogenous ALA by DT-infected host cells awaits further study, it is apparently made available to the intra-PV DTs, rendering them uroporphyric. The variability in the fluorescence intensity of URO in individual intra-PV DTs is not unexpected, considering the stochastic cellular events of uroporphyrinogenesis, as noted previously with ALA-exposed DT promastigotes (10).

The most significant finding of the present study is the host-parasite differential porphyrinogenesis, which is greatly in favor of the intra-PV amastigotes after pulse-exposure of the DT-infected cells to ALA. The host cells clearly utilize this exogenous ALA to overproduce porphyrins of the expected species, i.e., URO, COPRO, and PROTO, rendering them "visible" microscopically and chromatographically (Fig. 1 and 2). Other mammalian cells are known to undergo similar porphyrinogenesis by taking up exogenous ALA via their plasma membrane peptide transporters (28, 39). On removal of the exogenous ALA, the rapid loss of cellular porphyrins from the host cells is also expected, apparently accounted for in part by their release (16) and largely by their expected utilization for the formation of nonfluorescent products through the heme metabolic pathway (31). We observed such outcomes in all samples except the DT-infected cells, in which URO persists in the intra-PV DTs (Fig. 1A′ and 2), consistent with the observation of ALA-exposed DT promastigotes (10, 30). There is no apparent host-parasite transfer or exchange of the porphyrins overproduced by the respective cells. This is least likely for URO, since it is known to be released without reuptake by both *Leishmania* and mammalian cells (10). Any significant transfer of COPRO and/or PROTO from the host cells to intra-PV DTs would be expected to result in their persistence, since *Leishmania* has no enzymes to utilize these host-derived porphyrins. Taken together, the results suggest that the host cells and their DTs undergo independent porphyrinogenesis, almost certainly by using separate pools of ALA that are imported via different routes by the DT-infected cells.

Significantly, the host-parasite differential porphyrinogenesis after ALA pulse-exposure of the DT-infected cells makes it possible to achieve a selective accumulation of URO in the DTs, accounting for their specific susceptibility to photolysis (Fig. 3 to 5). There has been no report of such a strategy to selectively lyse intracellular parasites. The photosensitivity of the intra-PV uroporphyric DTs is such that their cytolysis is notable even when exposed to dim light (Fig. 3; see Fig. S2 in the supplemental material) and is extensive after experimental illumination under all conditions used (Fig. 4 to 6). Thus, effective photolysis of intra-PV uroporphyric DTs does not require a high fluence of illumination.

Another finding of equal importance in the present study is that the host cells remain viable and functional after ROS-mediated photolysis of their intra-PV uroporphyric DTs. This is not unexpected, considering that *Leishmania* normally resides in the phagolysosomes of macrophages, which are resistant to the ROS generated by their own respiratory burst (29). Indeed, the integrity and viability of the uroporphyric-DT-infected host cells is unaffected by the illumination conditions used. Timely illumination of infected cells when the uroporphyric DTs are already in the PVs/phagolysosomes, i.e., ~3 days after infection, produces optimal selectivity of DT photolysis. Although how the host cells detoxify the singlet oxygen expected to form immediately after light excitation of URO is unknown (10), they clearly return largely to

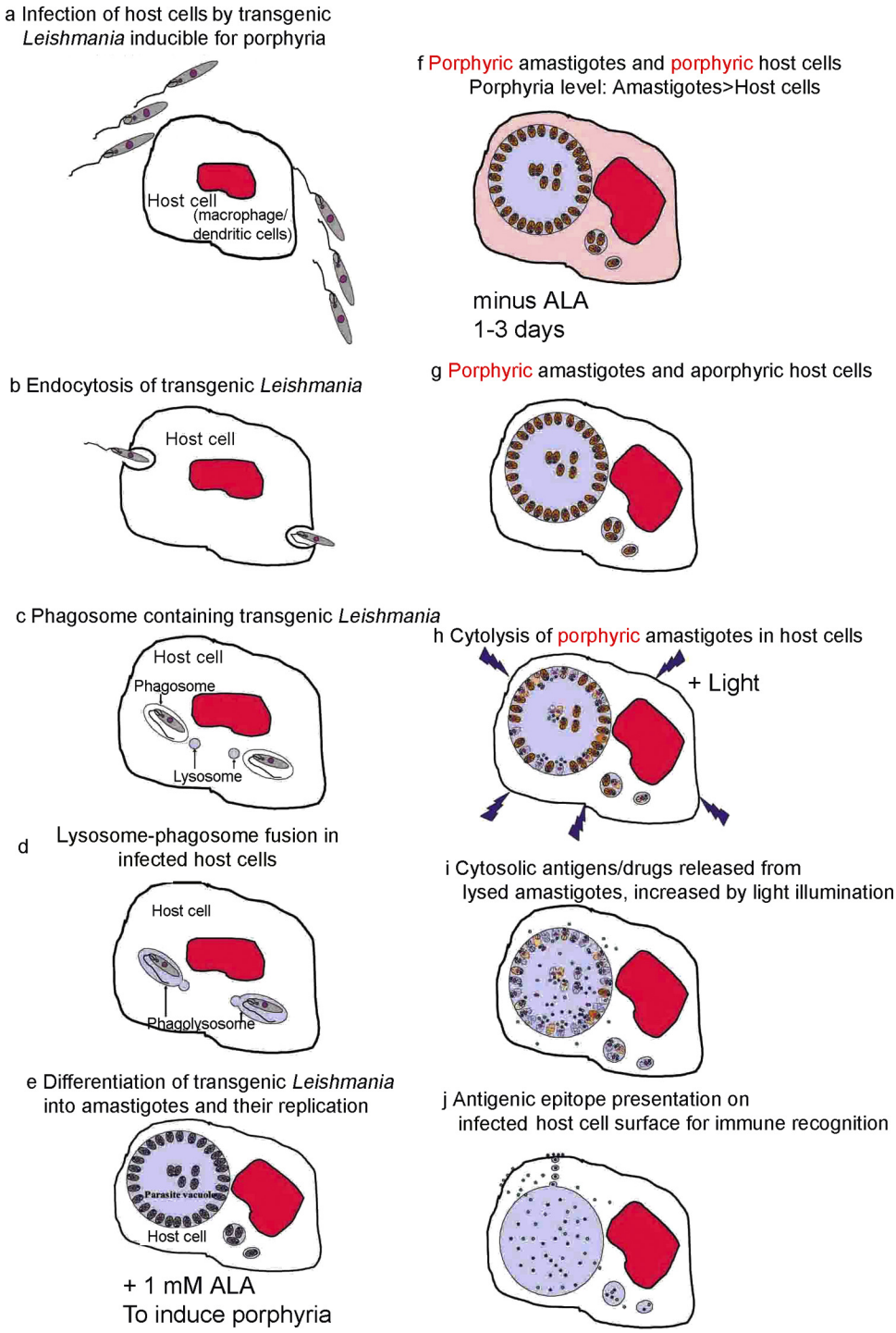

FIG 8 Schematic presentation of the cellular events involved in the use of *Leishmania* DT mutants as potential delivery vehicles of vaccines for photodynamic immunoprophylaxis and immunotherapy. (a to e) Sequential events during infection of host cells by porphyrinogenic mutants (DTs), as observed with wild-type *Leishmania*, leading to the establishment of intraphagolysosomal parasitism (cf. Fig. 1). (e to h) Pulse-exposure of DT-infected cells to ALA for selective accumulation of URO in the intra-PV DTs and their intralysosomal photolysis (cf. Fig. 2 to 5). (i to j) Drugs/vaccines (dots) hypothetically released from photolysed *Leishmania* cells (cf. Fig. 6 and 7).

their preinfection state, judging from their ability to maintain their integrity as a monolayer and to replicate subsequently (Fig. 3A′ and 4A′ and B′). This conclusion is supported by the microarray analysis assessed at a single time point. The expression profiles of the ~300 genes in the macrophages that are most affected by DT infection become increasingly similar to those of the uninfected host cells, consistent with decreasing levels of the parasite transcripts after uroporphyrinogenesis/photolysis (Fig. 7). Fur-

ther analyses of samples at additional time points may reveal a more complete reversal and the potential significance of the up- and downregulated cytokine transcripts (see the legends to Tables S1 and S2 in the supplemental material).

Most significantly, evidence is presented indicating that the cellular distribution of the MHC class II molecules returns to normal in macrophages after DT photolysis (Fig. 6; see Fig. S3 in the supplemental material). Infection of macrophages with *L. amazonensis* is known to sequester their MHC class II molecules in their residential phagolysosomes/PVs, thereby diminishing the capacity of these APCs for antigen presentation as a strategy of immune evasion (20, 23). Our observation is consistent with the previous report that these molecules are sequestered in the compartment between the parasite and the vacuolar membranes (2). Selective photolysis of the intra-PV uroporphyric DTs clearly restores the normal distribution of these molecules, suggestive of releasing these host cells from *Leishmania* immunosuppression.

In situ photolysis of uroporphyric DTs was shown to release antigens in dendritic cells for presentation via the MHC class I pathway. Transfection of DTs to express OVA as a model antigen makes it possible to demonstrate this antigen-presenting capacity by using a monoclonal antibody that recognizes an OVA SIIN FEKL peptide-MHC class I complex with specificity (see Fig. S5 in the supplemental material). The reaction products did not appear unless OVA-DTs were photolysed *in situ*, indicative of antigen processing and presentation. While this reactivity with the monoclonal antibody is not as intense as those with the peptide and OVA, the preliminary finding indicates the antigen-presenting capacity of this vaccine delivery system. Work is under way to optimize the experimental conditions for OVA antigen presentation to peptide-specific T cells along the line, as shown with phthalocyanine-loaded *Leishmania* as an alternative photolytic vaccine delivery vehicle (11).

The results presented strengthen our proposal that the uroporphyrinogenic DT is uniquely suitable as a carrier for drug/vaccine delivery (30). Figure 8 schematically summarizes this model to illustrate its potential advantages in photodynamic vaccination (22). First, the 2 transgenic products of the DTs produce no change in their ability to home to the phagolysosomes of APCs (Fig. 8a to d); hence, they are fully capable of protecting their potential payloads of drugs/vaccines *en route* to the desirable destination. The DTs thus differ from the metabolically or genetically compromised *Leishmania* parasites that were used previously for the same purpose after drug treatments (7) or after knocking out their housekeeping/infection-related genes (1, 33, 35, 38). Second, the DTs are signaled for lysis to release their payloads only after taking up residence in the relatively ROS-resistant phagolysosomes of infected APCs. This is made possible by induction of uroporphyrinogenesis for their selective photolysis (Fig. 8e to i), leaving the host cells viable and functional. Such treatments thus differ from the use of cytotoxic nucleoside analogues to kill *Leishmania* transfectants with suicide genes after immunization (8, 14, 25). Optimal recovery of the host cells, as shown in our case, may well be crucial, enabling them not only to be free of *Leishmania*-imposed immunosuppression, but also to adequately process antigens/vaccines released from the photolysed DTs for presentation to elicit effective immunity (Fig. 8i to j). This may account for the immune clearance of the few surviving DTs and for the prophylactic protection of animals against wild-type parasite challenges observed (22).

Work is ongoing to enhance the applicability of the DTs to vaccination. For example, transfection of DTs with luciferase was found to mediate the emission of luminescence in the vicinity of the cytosolic URO for their complete photolysis (unpublished data). Also, additional transfection of DTs with ALA synthase has the potential to render exogenous application of ALA unnecessary. Expression of these genes in constructs for amastigote stage-specific expression is also under way. As these transfectants reach macrophage phagolysosomes, their differentiation from promastigotes into amastigotes is thus expected to trigger uroporphyrinogenesis and emission of luminescence for automatic photolysis, thereby eliminating the need for externally supplied ALA and illumination. In the present study, the incomplete photolysis of the intraphagolysosomal uroporphyric DTs observed is not unexpected, as noted for the promastigote, due to the stochasticity of ALA-induced uroporphyrinogenesis (10). Previously, we presented evidence for the absence of DTs at the site of immunization after illumination *in situ*. Although their persistence elsewhere cannot be ruled out, the immunized animals developed a solid prophylactic immunity that was adoptively transferable to naïve animals (22). Whether the development of this immunity also cleared the residual DTs is unknown. More recently, prephotoinactivation of OVA transfectants sensitized with novel phthalocyanines was found to effectively deliver this model antigen to dendritic cells (DC4.2) for presentation of OVA to activate OVA peptide-specific $CD8^+$ T cells *in vitro* (11). Similar approach for uroporphyric DTs and synergistic photosensitization of these cells with novel phthalocyanines represents alternative strategies, which are under study, to produce effective but nonproliferating and nonviable vaccine carriers to ensure their safety margin. To serve as a universal platform, they could be engineered to express any of a variety of peptides for therapy/prophylaxis against other infectious and noninfectious diseases. The efficacy of these add-on drugs/vaccines may be enhanced by the adjuvant and other immunogenic activities of *Leishmania* endogenous molecules against diseases that are otherwise refractory to conventional approaches to prophylaxis and therapy.

ACKNOWLEDGMENTS

We thank John Keller for his critical review of the manuscript and suggestions.

This work is supported by NIH AI-20486 and AI-068835 and by Graduate and Postdoctoral Studies, Rosalind Franklin University (K.-P.C.).

REFERENCES

1. **Alexander J, Coombs GH, Mottram JC.** 1998. *Leishmania mexicana* cysteine proteinase-deficient mutants have attenuated virulence for mice and potentiate a Th1 response. J. Immunol. **161**:6794–6801.
2. **Antoine JC, Lang T, Prina E, Courret N, Hellio R.** 1999. H-2M molecules, like MHC class II molecules, are targeted to parasitophorous vacuoles of *Leishmania*-infected macrophages and internalized by amastigotes of *L. amazonensis* and *L. mexicana.* J. Cell Sci. **112**:2559–2570.
3. **Chang CS, Chang KP.** 1985. Heme requirement and acquisition by extracellular and intracellular stages of *Leishmania mexicana amazonensis.* Mol. Biochem. Parasitol. **16**:267–276.
4. **Chang KP, Fong D.** 1983. Cell biology of host-parasite membrane interactions in leishmaniasis. Ciba Found. Symp. **99**:113–137.
5. **Chen DQ, et al.** 2000. Episomal expression of specific sense and antisense mRNAs in *Leishmania amazonensis*: modulation of gp63 level in promastigotes and their infection of macrophages *in vitro.* Infect. Immun. **68**:80–86.
6. **Chen JW, Cha Y, Yuksel KU, Gracy RW, August JT.** 1988. Isolation and sequencing of a cDNA clone encoding lysosomal membrane glycoprotein

mouse LAMP-1. Sequence similarity to proteins bearing oncodifferentiation antigens. J. Biol. Chem. **263**:8754–8758.
7. **Daneshvar H, et al.** 2010. Gentamicin-attenuated *Leishmania infantum*: cellular immunity production and protection of dogs against experimental canine leishmaniasis. Parasite Immunol. **32**:722–730.
8. **Davoudi N, et al.** 2005. Development of a recombinant *Leishmania major* strain sensitive to ganciclovir and 5-fluorocytosine for use as a live vaccine challenge in clinical trials. Vaccine **23**:1170–1177.
9. **Dutta S, Furuyama K, Sassa S, Chang KP.** 2008. *Leishmania* spp.: delta-aminolevulinate-inducible neogenesis of porphyria by genetic complementation of incomplete heme biosynthesis pathway. Exp. Parasitol. **118**:629–636.
10. **Dutta S, Kolli BK, Tang A, Sassa S, Chang KP.** 2008. Transgenic *Leishmania* model for delta-aminolevulinate-inducible monospecific uroporphyria: cytolytic phototoxicity initiated by singlet oxygen-mediated inactivation of proteins and its ablation by endosomal mobilization of cytosolic uroporphyrin. Eukaryot. Cell **7**:1146–1157.
11. **Dutta S, et al.** 2011. Intracellular targeting specificity of novel phthalocyanines assessed in a host-parasite model for developing potential photodynamic medicine. PLoS One **6**:e20786.
12. **Dutta S, Ray D, Kolli BK, Chang KP.** 2005. Photodynamic sensitization of *Leishmania amazonensis* in both extracellular and intracellular stages with aluminum phthalocyanine chloride for photolysis *in vitro*. Antimicrob. Agents Chemother. **49**:4474–4484.
13. **Eisen MB, Spellman PT, Brown PO, Botstein D.** 1998. Cluster analysis and display of genome-wide expression patterns. Proc. Natl. Acad. Sci. U. S. A. **95**:14863–14868.
14. **Ghedin E, et al.** 1998. Inducible expression of suicide genes in *Leishmania donovani* amastigotes. J. Biol. Chem. **273**:22997–23003.
15. **Girolomoni G, et al.** 1995. Establishment of a cell line with features of early dendritic cell precursors from fetal mouse skin. Eur. J. Immunol. **25**:2163–2169.
16. **Hamza I.** 2006. Intracellular trafficking of porphyrins. ACS Chem. Biol. **1**:627–629.
17. **Hunter GA, Ferreira GC.** 2011. Molecular enzymology of 5-aminolevulinate synthase, the gatekeeper of heme biosynthesis. Biochim. Biophys. Acta. doi:10.1016/j.bbapap.2010.12.015.
18. **Kari L, et al.** 2003. Classification and prediction of survival in patients with the leukemic phase of cutaneous T cell lymphoma. J. Exp. Med. **197**:1477–1488.
19. **Kelty CJ, Brown NJ, Reed MW, Ackroyd R.** 2002. The use of 5-aminolaevulinic acid as a photosensitiser in photodynamic therapy and photodiagnosis. Photochem. Photobiol. Sci. **1**:158–168.
20. **Kima PE, Soong L, Chicharro C, Ruddle NH, McMahon-Pratt D.** 1996. *Leishmania*-infected macrophages sequester endogenously synthesized parasite antigens from presentation to CD4+ T cells. Eur. J. Immunol. **26**:3163–3169.
21. **Krammer B, Plaetzer K.** 2008. ALA and its clinical impact, from bench to bedside. Photochem. Photobiol. Sci. **7**:283–289.
22. **Kumari S, et al.** 2009. Photodynamic vaccination of hamsters with inducible suicidal mutants of *Leishmania amazonensis* elicits immunity against visceral leishmaniasis. Eur. J. Immunol. **39**:178–191.
23. **Lang T, et al.** 1994. Distribution of MHC class I and of MHC class II molecules in macrophages infected with *Leishmania amazonensis*. J. Cell Sci. **107**:69–82.
24. **McMahon-Pratt D, Alexander J.** 2004. Does the *Leishmania major* paradigm of pathogenesis and protection hold for New World cutaneous leishmaniases or the visceral disease? Immunol. Rev. **201**:206–224.
25. **Muyombwe A, et al.** 1998. Protection against *Leishmania major* challenge infection in mice vaccinated with live recombinant parasites expressing a cytotoxic gene. J. Infect. Dis. **177**:188–195.
26. **Opperdoes FR, Coombs GH.** 2007. Metabolism of *Leishmania*: proven and predicted. Trends Parasitol. **23**:149–158.
27. **Ralph P, Nakoinz I.** 1975. Phagocytosis and cytolysis by a macrophage tumour and its cloned cell line. Nature **257**:393–394.
28. **Rodriguez L, et al.** 2006. Study of the mechanisms of uptake of 5-aminolevulinic acid derivatives by PEPT1 and PEPT2 transporters as a tool to improve photodynamic therapy of tumours. Int. J. Biochem. Cell Biol. **38**:1530–1539.
29. **Roos D.** 1991. The involvement of oxygen radicals in microbicidal mechanisms of leukocytes and macrophages. Klin. Wochenschr. **69**:975–980.
30. **Sah JF, et al.** 2002. Genetic rescue of *Leishmania* deficiency in porphyrin biosynthesis creates mutants suitable for analysis of cellular events in uroporphyria and for photodynamic therapy. J. Biol. Chem. **277**:14902–14909.
31. **Sassa S.** 2006. The hematologic aspects of porphyria, p 803–822. *In* Lichtman MA, et al. (ed), Williams hematology, 7th ed. McGraw-Hill, Inc., New York, NY.
32. **Sassa S, Nagai T.** 1996. The role of heme in gene expression. Int. J. Hematol. **63**:167–178.
33. **Selvapandiyan A, et al.** 2009. Intracellular replication-deficient *Leishmania donovani* induces long lasting protective immunity against visceral leishmaniasis. J. Immunol. **183**:1813–1820.
34. **Snyderman R, Pike MC, Fischer DG, Koren HS.** 1977. Biologic and biochemical activities of continuous macrophage cell lines P388D1 and J774.1. J. Immunol. **119**:2060–2066.
35. **Titus RG, Gueiros-Filho FJ, de Freitas LA, Beverley SM.** 1995. Development of a safe live *Leishmania* vaccine line by gene replacement. Proc. Natl. Acad. Sci. U. S. A. **92**:10267–10271.
36. **Trager W.** 1974. Nutrition and biosynthetic capabilities of flagellates: problems of *in vitro* cultivation and differentiation, p 225–245. *In* Trypanosomiasis and leishmaniasis with special reference to Chagas' disease. CIBA Foundation Symposium 20 (new series). Elsevier, Amsterdam, The Netherlands.
37. **Tusher VG, Tibshirani R, Chu G.** 2001. Significance analysis of microarrays applied to the ionizing radiation response. Proc. Natl. Acad. Sci. U. S. A. **98**:5116–5121.
38. **Uzonna JE, Späth GF, Beverley SM, Scott P.** 2004. Vaccination with phosphoglycan-deficient *Leishmania major* protects highly susceptible mice from virulent challenge without inducing a strong Th1 response. J. Immunol. **172**:3793–3797.
39. **Xiang J, Hu Y, Smith DE, Keep RF.** 2006. PEPT2-mediated transport of 5-aminolevulinic acid and carnosine in astrocytes. Brain Res. **1122**:18–23.
40. **Zhao B, He YY.** 2010. Recent advances in the prevention and treatment of skin cancer using photodynamic therapy. Expert Rev. Anticancer. Ther. **10**:1797–1809.